

---

This item was submitted to [Loughborough's Research Repository](#) by the author.  
Items in Figshare are protected by copyright, with all rights reserved, unless otherwise indicated.

## **Infrared monitoring of aluminium milling processes for reduction of environmental impacts**

PLEASE CITE THE PUBLISHED VERSION

<http://www.irjes.com/Papers/vol6-issue6/B6610821.pdf>

PUBLISHER

IRJES

VERSION

VoR (Version of Record)

PUBLISHER STATEMENT

This work is made available according to the conditions of the Creative Commons Attribution 4.0 International (CC BY 4.0) licence. Full details of this licence are available at: <http://creativecommons.org/licenses/by/4.0/>

LICENCE

CC BY 4.0

REPOSITORY RECORD

Simeone, Alessandro, Elliot Woolley, Yang Luo, Owain Williams, and Shahin Rahimifard. 2019. "Infrared Monitoring of Aluminium Milling Processes for Reduction of Environmental Impacts". figshare. <https://hdl.handle.net/2134/24094>.

## Infrared Monitoring of Aluminium Milling Processes for Reduction of Environmental Impacts

Alessandro Simeone<sup>1</sup>, Elliot Woolley<sup>1</sup>, Yang Luo<sup>1</sup>, Owain Williams<sup>1</sup>,  
Shahin Rahimifard<sup>1</sup>

<sup>1</sup>Centre for Sustainable Manufacturing and Recycling Technologies, Wolfson School Of Mechanical, Electrical  
And Manufacturing Engineering, Loughborough University, LE11 3YUUK

**Abstract:**-In modern manufacturing contexts, process monitoring is an important tool aimed at ensuring quality standard fulfilment whilst maximising throughput. In this work, a monitoring system comprised of an infrared (IR) camera was employed for tool state identification and surface roughness assessment with the objective of reducing environmental impacts of a milling process. Two data processing techniques, based on statistical parameters and polynomial fitting, were applied to the temperature signal acquired from the IR camera during milling operations in order to extract significant features. These features were inputted to two different neural network based procedures: pattern recognition and fitting, for decision making support on tool condition and surface roughness evaluation respectively. These capabilities are discussed in terms of reducing waste products and energy consumption whilst further improving productivity.

**Keywords:**infrared monitoring, eco-intelligent manufacturing, milling, neural networks, artificial intelligence

### I. INTRODUCTION

Recent decades have seen a growing understanding of the environmental impacts associated with global manufacturing activities, resulting in a developing field of research which seeks to reduce these impacts. Such research has, for example, targeted improvements in manufacturing energy efficiency [1]–[3] since this industry has been identified as a significant contributor to atmospheric greenhouse gases and their associated ramifications on global climate. Equivalent research on material efficiency, water consumption, and the generation of solid, liquid and other airborne waste streams, amongst others, have also become prevalent. The current body of research into reducing environmental impacts typically seeks to fully understand the various factors before developing a strategy to reduce them via either: i) physical changes to products or processes to improve efficiency or reduce waste; or ii) through operational or control improvements that seek to use the existing infrastructure more effectively. Clearly the first of these two options typically requires longer term investment, changes of equipment or process and is therefore more costly, whilst the second is easier, but may be more challenging when attempting to achieve more than incremental improvements.

This research is concerned with the second of these two approaches, which can be easily implemented and yield early results, whilst physical changes can be implemented over longer time periods. However, any reduction in environmental impact must also preserve and enhance speed, quality or practicability of manufacturing products. In this context, there is the opportunity to extract information from data acquired from a diverse range of manufacturing processes, and use this to actively control operational parameters to improve the environmental performances of these processes. In this work infrared monitoring is used to investigate an aluminium milling process with the objective of reducing the amount of material and energy required for processing through the following improvements: prevention of rejects from defects (particularly for high value manufacturing); ensuring quality to prevent re-work; avoidance of excessive tool wear; fulfilment of surface integrity requirements; prediction and prevention of catastrophic failures; and reduction in processing time. All of these improvements not only reduce the environmental impact of the processes, but also are in line with the current manufacturing objectives of increasing speed, quality, reliability and cost effectiveness.

In this paper a literature review is reported covering sustainable machining, sensor monitoring of machining processes, tool wear assessment and surface roughness modelling. The experimental work and the equipment utilised are described. Data processing procedures are illustrated, consisting of feature extraction and the development of a decision making support system. The results are reported and discussed from two perspectives: the tool state identification and surface roughness assessment. An important objective for sustainable machining is improving efficiency in resource utilisation and raw materials extraction. It is necessary to improve the proportion between incoming raw materials and outgoing products during the production phase which implies reducing waste and eliminating mechanical and chemical degradation of machined surface [1].

At present, the environmental factors associated with manufacturing processes have become an emerging problem for manufacturers due to stricter regulations on wastes, effluents, emissions, health and workers' safety [4]. Therefore, in parallel with manufacturing process optimisation, efforts must be made to reduce the impact of industrial activity on environment and health [5]. Tool Condition Monitoring (TCM) is an essential part of automating modern machining processes to ensure efficiency and minimise waste [6]. The work of Teti et al. [7] gives a comprehensive overview of this area. The approaches to TCM are categorised as either "direct" or "indirect"; for direct monitoring the tool wear is measured optically or physically, whereas for indirect monitoring another, more accessible quantity is measured, then used to deduce the tool wear [8]. Common indirect measurement quantities include: cutting forces, power, temperature rise, work piece surface finish, vibration, and chatter [8]. Whilst direct methods often show the best accuracy, their use is typically restricted to the laboratory, due to practical access and illumination problems in industrial environments [7]. An example of such an approach is that of Kerr et al. [9], who used digital image processing techniques on a close-up video image of a tool to monitor "on-line" tool wear (whilst the machine is running). It is vital for practical use in industry that any TCM system must be on-line, to prevent wasted manufacturing time [6]. For indirect measurements, this is made easier by the fact that the measurand can be selected such that it is not obscured by the work piece, chips, or cutting fluid. Often several quantities are measured simultaneously, such as in the work by Segreto et al. [10], who correlated measurements of force, vibration and Acoustic Emission (AE) to the wear level in a turning operation, or [11] who used pressure, force, vibration and AE to assess the tool condition in broaching operations.

One key area of research in indirect TCM relates to the measurement of temperature. As first recognised by Taylor in 1907 [12], [13] this is a particularly important "tool wear indicator" [6], as heat build-up is both a symptom and a contributing factor to tool wear [12], [13]. High temperatures in machining can cause problems in the work piece as well, including poor dimensional accuracy and surface finish, and residual stresses [12]. A thorough overview of the monitoring of temperature in material removal processes can be found in the work of Davies et al. [12]. Common approaches to the measurement of temperature for TCM include the use of resistance methods, thermocouples (such as that by Kitagawa et al. [14] and thermo-physical processes; however, the approach that currently has the best spatial and temporal resolution is the use of "Spectral Radiation Thermometry" (infrared monitoring) [12], [15]. This method, exploiting the correlation between the temperature of an object and the wavelength of the electromagnetic radiation energy that it emits, has a number of other significant advantages for the monitoring of machining processes. Chief amongst these is the remote nature of the measurement method, meaning that no holes or sensors need to be incorporated into the cutting tool, which might affect the accuracy of reading [12], [13]. This technique also looks at the local surface temperatures on the faces and edges of the cutting tool, which are more important than the average temperatures in the tool when considering tool wear [15].

Surface properties strongly influence the performance of a finished part. They have an enormous impact on features such as dimensional accuracy, friction coefficient and wear, thermal and electric resistance, fatigue limit, corrosion, post-processing requirements, appearance and cost [16]. The measurement of the surface roughness is commonly carried out off-line when the part is already machined [16] and it is often used as an acceptability criterion for mechanical products [17]. A review of literature highlights a wide research focused on surface generation to understand the process and provide the necessary knowledge to guarantee surface quality before the start of the metal removal operation. In terms of intelligent decision making support systems, neural network approach is surely one of the most reported methodologies. In particular, for surface roughness assessment applications, Anuj Kumar [18] describes a model for surface roughness prediction for turning of rolled aluminium. The model is tested by using the Analysis of variance (ANOVA) and an Artificial Neural Network analysis is adopted with the experimental values as input-output pairs. Otkem et al. [19] presents an approach for determination of the best cutting parameters leading to minimum surface roughness in end milling mould surfaces by coupling a genetic algorithm with neural network. Two techniques, namely factorial design and neural network were used in the work of Esme et al [20] for modelling and predicting the surface roughness of AISI 4340 steel.

Literature also details a range of research comprising the use of neural networks applied on sensor data aimed at surface roughness assessment. Benardos and Vosniakos [17] propose a neural network modelling approach for SRP in face milling. The factors considered in the experiment were the depth of cut, the feed rate per tooth, the cutting speed, the engagement and wear of the cutting tool, the use of cutting fluid and the three components of the cutting force. An on-line surface recognition system was developed by Lee and Chen [21] based on artificial neural networks using a sensing technique to monitor the effect of vibration produced by the motions of the cutting tool and workpiece during turning processes. Tsai et al. [22] developed an in-process based surface recognition system. An accelerometer and a proximity sensor were employed during cutting to collect the vibration and rotation data, respectively. An artificial neural networks model was developed to predict the roughness values. Risbood et al. [23] using neural networks, predicted surface roughness within a

reasonable degree of accuracy by taking the acceleration of radial vibration of tool holder as a feedback. An intelligent sensor fusion technique to estimate on-line surface roughness during steel turning was proposed by Azouzi and Guillot[24] who utilised a dynamometer, an accelerometer, an acoustic emission transducer and two capacitance sensors to build a neural network based decision making support system.

Another technique of surface roughness prediction has been developed by Aguiar et al. [25] using multi-sensor method with an AE sensor and power meter for grinding process. Acoustic emission and cutting power signals are shown to be very good input parameters to the neural network for surface roughness prediction of ground parts. Neural networks have the capability to analyse a number of measurements from a machining operation to provide data regarding a seemingly unrelated parameter. This removes the need for direct measurements and opens up opportunities for low cost, remote sensing technologies to provide critical data about machining condition and performance. To meet the need of manufacturers to reduce their environmental impacts, from the excessive use of energy and time, and to reduce the occurrence of sub-standard parts production, the current research is concerned with the use of remote sensing to determine tool bit and work piece condition, to better manage these impacts in real time.

## II. MATERIALS AND EXPERIMENTAL PROCEDURES

Among several CNC industrial machining processes, milling is a fundamental machining operation. End milling is the most common metal removal operation encountered and is widely used in a variety of manufacturing industries including the aerospace and automotive sectors, where quality is an important factor in the production of slots, pockets, precision moulds and dies [26]. Hence in this research, an end milling process was selected to be monitored by use of an infrared camera for detection of tool wear state and surface finish.

The cutting experiments were carried out on a XYZ SMX2000 CNC three-axis vertical milling machine, with a 2.25 kW drive motor, and a maximum spindle speed of 4200 RPM. This allowed for accurate control of the machining feed rate and spindle speed, whilst maintaining simplicity and ease of access for the infrared camera. Two Sherwood four-toothed, 12mm diameter end mills were used, made of M2 High Speed Steel (HSS). One of these was in a “worn” state, having been used for standard machining processes on both steel and aluminium; the other was unused. The work piece material was square stock, 6068 Aluminium, measuring 51 x 51 x 610 mm. All the machining operations were done under “dry” cutting conditions. This condition was chosen to ensure clean and clear results, as the addition of coolant or lubricant was found to interfere with the thermographic image, and dramatically reduce the temperature in the relatively low-temperature machining of aluminium. This “dry” condition is common to many similar investigations, such as Lauro et al. [27], Kodácsy&Molnár[28] and Kitagawa et al. [14]. The tool was, however, allowed to cool to room temperature between tests to ensure a constant starting temperature.

**Table 1.** Cutting conditions for milling tests

Cutting conditions	
<b>Work piece Material</b>	6068 Aluminium
<b>Cutting Tool</b>	End mill
	Material: HSS M2
<b>Tool Geometry</b>	Diameter: 12 mm
	30° Helix, 4 flutes
<b>Conditions</b>	Dry. Tool allowed to cool to room temperature between each test
<b>Wear criterion</b>	VB> 0.3 mm
<b>Depth of cut</b>	0.5 mm



**Figure 1.** Experimental setup

A range of feed rate and spindle speed process parameters were investigated during the experimental procedure, in order to evaluate their effect on the ability of the system to identify wear. The cut depth was fixed at 0.5 mm. The chosen experimental parameters are summarised in Table 2. These were chosen based upon the recommended speeds and feeds for the tool and work piece materials, adjusted due to the dry conditions. One of the most critical causes of tool wear in the dry machining of aluminium is the build-up of material on the tool, caused by excessive temperatures [6]. The lower feed rates, cut depth and spindle speeds were therefore chosen to avoid this situation, which would otherwise skew the results. The feed rates adopted were respectively 254, 508 and 762 mm/min while the cutting speeds selected were 900 1200 and 1500 rpm. Fig. 1 shows the experimental setup used. The data acquisition was done using a Cedip Infrared Systems Silver 450M InSb type infrared camera, with a frame rate of 383 per second, and a calibration range of 5 to 300 °C.

Before commencing the experimental procedure, it was important to confirm quantitatively that the fresh and worn tools were in the expected state prior to machining, and that the wear on the fresh tool remained negligible throughout. The criteria used for determining the point at which a tool became worn was the same as that used by Azmi[29], who defined an end mill cutting tool as worn when it exhibited any of the following: “reach maximum uniform flank wear, VBmax of 0.3 mm on any cutting flute, or reach an average flank wear, VB of 0.3 mm on all four cutting flutes, or excessive edge, nose deformation/rounding or chipping on more than 2 cutting flutes.” This is confirmed by Kalpakjian and Schmid[8], who define the average allowable wear land (VB) for end milling to be 0.3 mm. For these tests, this was measured using a SmartScope Flash 200 automatic measurement system, accurate to approximately 2 µm. It is to be noted that this criteria does not take into account catastrophic wear, but accounts for common wear in normal usage. The recorded values for the wear of the worn tool also represent a minimum value for the wear as the original point that they would have been measured relative to was chipped, or worn away. They are, however, sufficient to show the worn tool to have surpassed the wear criteria (0.3 mm), and that the wear on the fresh tool remained well below 0.1 mm throughout.

**Table 2.** Design of the experiments

Feed Rate (mm / min)	Cutting Speed (RPM)	Test ID Fresh Tool	Test ID Worn Tool
254	900	T 1 Fresh 1	T 1 Worn 1
		T 1 Fresh 2	T 1 Worn 2
254	1200	T 2 Fresh 1	T 2 Worn 1
		T 2 Fresh 2	T 2 Worn 2
254	1500	T 3 Fresh 1	T 3 Worn 1
		T 3 Fresh 2	T 3 Worn 2
508	900	T 4 Fresh 1	T 4 Worn 1
		T 4 Fresh 2	T 4 Worn 2
508	1200	T 5 Fresh 1	T 5 Worn 1
		T 5 Fresh 2	T 5 Worn 2
508	1500	T 6 Fresh 1	T 6 Worn 1
		T 6 Fresh 2	T 6 Worn 2
762	900	T 7 Fresh 1	T 7 Worn 1
		T 7 Fresh 2	T 7 Worn 2
762	1200	T 8 Fresh 1	T 8 Worn 1
		T 8 Fresh 2	T 8 Worn 2
762	1500	T 9 Fresh 1	T 9 Worn 1
		T 9 Fresh 2	T 9 Worn 2

**Table 3.** IR Thermography Input Conditions

IR thermography input conditions	
Tool emissivity	0.393
Distance to tool	0.91 m
Atmospheric temperature	22 °C
Reflected temperature	22 °C

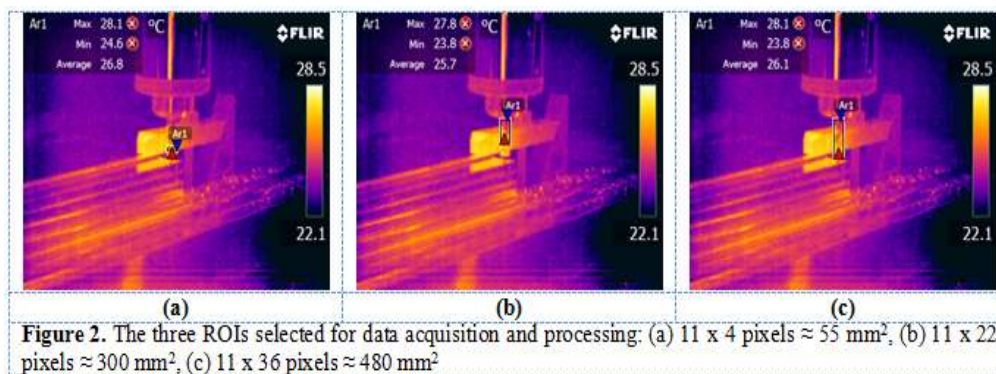
In order to take practical, but accurate measurements of the temperature of an object using infrared monitoring its emissivity must be known. This is a complicated parameter, depending on a range of factors, including the temperature, material and surface finish of the measured object [15]; this, in itself is a simplification (the “grey body” assumption [12]), as the emissivity can also vary with both wavelength and direction [15]. However, a practical value for emissivity was derived by synchronous measurement of the temperature of the cutting tool using both the infrared camera and a K-type thermocouple over a range of temperatures, as delivered using a hot air gun. This is similar to the approaches used by a number of other authors [7], [14]–[16]. A similar, although more thorough approach to emissivity calibration was taken by Valiorgue et al. [15], who integrated the emissivity curve with the IR radiation measurements over a full range of temperatures in order to account for the dependence of emissivity on temperature.

In this work, once these values were acquired, the optimisation function in Microsoft Excel was used to select a value for emissivity that most closely matched the IR camera readings to those recorded using the thermocouple; the emissivity coefficient and the other influencing factors on the IR camera temperature reading are summarised in Table 3.

### III. DATA PROCESSING AND FEATURES EXTRACTION

#### 3.1 Data Pre-Processing

The temperature signals used for analysis were extracted from the recorded IR film using FLIR’s “ResearchIR” software. Within the infrared video acquired during the cutting tests, Regions of Interest (ROIs) are defined in order to retrieve signals related to the zones of interest. Three different rectangular ROIs were chosen to investigate the tool-chip interface area: 11 x 4 pixels, 11 x 22 pixels and 11 x 36 pixels respectively as shown in Figure 2 [30]. A number of advantages are gained by this approach: firstly, by averaging over an area, the temperature spike effect of flying chips intersecting with the field of measurement [6] is reduced; secondly, by looking at an area slightly removed from the tool-work piece interface, any “dazzle” from the high infrared radiation output at the interface is minimised, which might otherwise skew the results [15], [27]. However, the positioning was chosen to still be sufficiently close to the interface that the response time to changing temperatures would be kept low.



This positioning also meant that the temperature drop was not excessively low, which was important to maintain a high “Noise Equivalent Temperature Ratio” – the “noise” in this case being the heating and cooling cycle due to the intermittent nature of milling cutting [14]. For each ROI, a signal segmentation procedure was implemented on the raw infrared signals, by trimming the signal, to include only the segment where the tool is in contact with the workpiece, as shown in Figure 3. This operation was performed on each milling test signal.

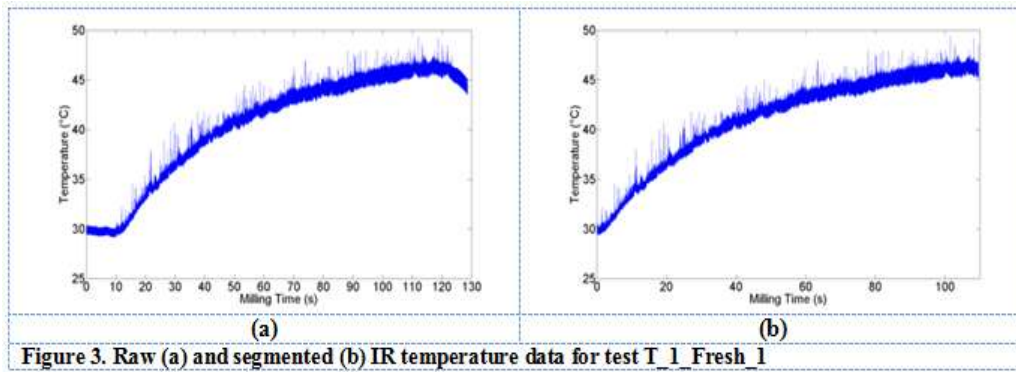


**Figure 3. Raw (a) and segmented (b) IR temperature data for test T\_1\_Fresh\_1**

### 3.2 Dataset Preparation

A data set is a matrix whose rows are represented by a certain number of samplings with the columns corresponding to the 36 milling tests. Four different data sets were prepared, consisting of 1000, 2000, 4000 and 7500 rows (samplings) respectively. In Table 5 an example of 7500-samplings dataset is reported.

### 3.3 Features Extraction

The extraction of signal characteristic features from sensing systems is of primary importance in many information processing fields such as pattern recognition, predictive modelling, industrial process fault diagnosis and control, etc. [7], [31].

The statistical features are used for the proven effectiveness [32] and for the computational ease, since they do not require strong computational efforts and are suitable for real time monitoring. The polynomial features are used as an alternative to the statistical features in order to compare them and evaluate the results.

**Table 4. 7500 Samplings dataset**

Samplings	T_1_Fresh_1	T_1_Fresh_2	...	T_9_Worn_1	T_9_Worn_2
1	29.5097	30.0168	...	31.6677	32.8816
2	29.8423	30.0033	...	31.3615	33.5475
...	...	...	...	...	...
7500	36.5076	34.4815	...	50.1302	52.1439

In this paper two methodologies were adopted to extract features:

#### 3.1.1 Statistical Features

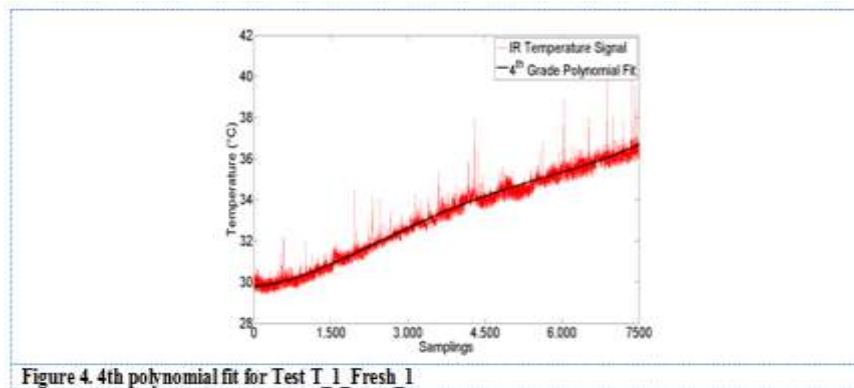
**Four statistical features were extracted from the segmented signal of each test:**

- Mean value
- Variance
- Skewness
- Kurtosis

The four statistical features mentioned above were grouped into feature vectors to be used as input to a neural network based decision making system [32].

#### 3.1.2 Polynomial Features

An alternative approach to the statistical features extraction is proposed in this paper. For each milling test, the coefficients of the polynomial  $p(x)$  of degree 4 that fits the IR temperature signal in a least squares sense, have been calculated. An example of 4th degree polynomial fitting is reported in Fig. 4 for Test T\_1\_Fresh\_1.



The result is 5 elements feature vector containing the polynomial coefficients in descending powers:

$$p(x) = \alpha x^4 + \beta x^3 + \gamma x^2 + \delta x + \varepsilon$$

Therefore a set of 5 features, the polynomial coefficients, was extracted from the segmented signal of each milling test:  $[\alpha \beta \gamma \delta \varepsilon]$ .

The infrared data processing and features extraction procedure can be summarised in Table 5.

**Table 5** Summary Of Signal Processing And Features Extraction Procedure

		1. ROIs definition							
		11 x 4 px	11 x 22 px	11 x 36 px					
Pre Processing		2. Segmentation							
		3. Dataset construction							
		1000 samplings	2000 samplings	4000 samplings	7500 samplings				
		4. Features Extraction							
Signal Processing		StatisticalFeatures		4 <sup>th</sup> degreePolynomial Coefficients					
		Mean	Variance	Skewness	Kurtosis	$\alpha$	$\beta$	$\gamma$	$\delta$

### 3.1 Neural Network based decision making support system

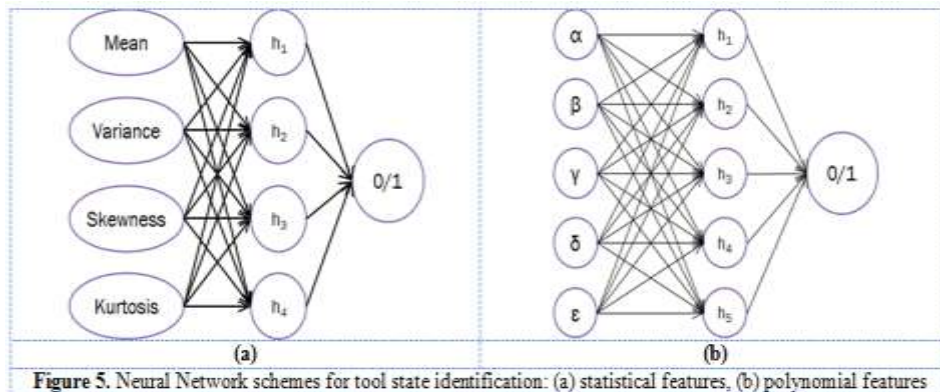
The features vectors obtained with the two methodologies were used to construct feature vectors to input to a neural network (NN) based pattern recognition procedure [7], [33] for decision making on tool wear state identification as well as to a neural network based fitting procedure for surface roughness assessment.

### 3.2 Neural Network Pattern Recognition for Tool State Identification

The feed-forward (FF) back-propagation (BP) NN is the most commonly used family of NN for pattern classification purposes [34]. Its structure is made of three layers (input, hidden and output layer respectively) as shown in Fig 5.

In this application the following NN architecture configurations were adopted:

- The number of input nodes was equal to the number of input features vector elements:
  - 4 nodes for statistical features as the feature vector is made of 4 elements: Mean, Variance, Skewness and Kurtosis.
  - 5 nodes for polynomial features as the features vector elements are the polynomial coefficients  $\alpha$ ,  $\beta$ ,  $\gamma$ ,  $\delta$  and  $\varepsilon$
- The number of hidden layer nodes is equal to the number of input layer nodes.
- The output layer had only 1 node, yielding a binary value associated with the tool wear state: 0 = fresh tool; 1 = worn tool.



### 3.3 Training, validation and testing

The FF BP NN learning algorithm adopted in this work was the Levenberg-Marquardt algorithm [35], [36] which is considered one of the fastest methods for learning moderate-sized FF BP NN [34]. The algorithm's principal mode of action is to find the minimum of a multiple variable function, which is expressed in the form of the sum of squares of nonlinear real-valued functions making it an iterative procedure and it is mostly used for nonlinear optimisation tasks [34], [35]. Data division for Levenberg-Marquardt training algorithm was carried out randomly with the following percentages: 70% of test cases were used for training; 15% for validation; 15% for testing.

The input matrix is composed of a number of rows equal to the number of test cases i.e. 36, and a number of columns equal to the number of elements of the input feature vectors (4 for statistical features and 5 for polynomial features). During testing, the NN output is correct if the error  $E = (O_a - O_d)$ , where  $O_a$  is equal to the actual output and  $O_d$  is equal to the desired output, is  $-0.5 \leq E \leq +0.5$ ; otherwise, a misclassification case occurs. The ratio of correct classifications over total training cases yields the NN success rate (SR).

### 3.4 Neural network fitting for surface roughness assessment

Roughness Measurements were carried out using a Taylor Hobson roughness device at the end of each milling test on the workpiece surface. The roughness parameter considered in this work was the average roughness ( $R_a$ ) reported for each test in Table 6.  $R_a$  is the arithmetic mean of the absolute departures of the roughness profile from the mean line. It is universally recognised and is the most often used international parameter of roughness [37], it is defined by the formula below:

$$R_a = \frac{1}{l} \int_0^l |z(x)| dx$$

**Table 6.** Surface roughness measurements

ID Test	Ra (µm)	ID Test	Ra (µm)
T_1_Fresh_1	4.03	T_1_Worn_1	0.48
T_2_Fresh_1	2.01	T_2_Worn_1	0.71
T_3_Fresh_1	3.86	T_3_Worn_1	0.53
T_4_Fresh_1	8.20	T_4_Worn_1	1.10
T_5_Fresh_1	4.75	T_5_Worn_1	1.48
T_6_Fresh_1	4.09	T_6_Worn_1	0.59
T_7_Fresh_1	9.93	T_7_Worn_1	2.89
T_8_Fresh_1	7.99	T_8_Worn_1	1.09
T_9_Fresh_1	5.03	T_9_Worn_1	1.22

The input matrices used for tool state identification were used also for surface roughness assessment. Two configuration of hidden layer nodes number were utilised for each set of input layer nodes, respectively:

- 8 and 16 hidden layer nodes for the 4 statistical input features
- 6 and 18 hidden layer nodes for the 5 polynomial features
- The output layer had only one node containing the  $R_a$  value (in µm).

For the evaluation of the generalisation ability of the trained neural network a linear fit between the output of the model and the experimental data for all the measured values presented in Table 6 was performed. The fitness indicator is hence the regression coefficient R-value.

#### IV. RESULTS AND DISCUSSION

##### 4.1 Tool state identification

The success rate was calculated for both the features extraction methodologies and for the three ROIs applied to the four datasets and illustrated in Figure 6. Results show that SR range from 85.01% to 98.61%, the average success rate of all the NN configurations is 93.73%, demonstrating the capability of both features extraction methodologies in generating valuable features for tool condition monitoring. The results reported in Figure 6 show that statistical features always yield a higher success rate compared to the polynomial features.

The best success rates were obtained using the 11x36 px ROI, with an average SR equal to 94.30%. Using 11x4 px ROI, the average SR slightly decreases to 93.72% while SR=90.17% is obtained using 11x22 px ROI. The success rate increases as the number of processed samplings increases. However, by considering 1000 samplings (2.6 seconds milling time) the tool state identification is performed with a very high success rate (85.01% – 91.65%), showing a quick response of infrared temperature signals for identifying the tool wear state.

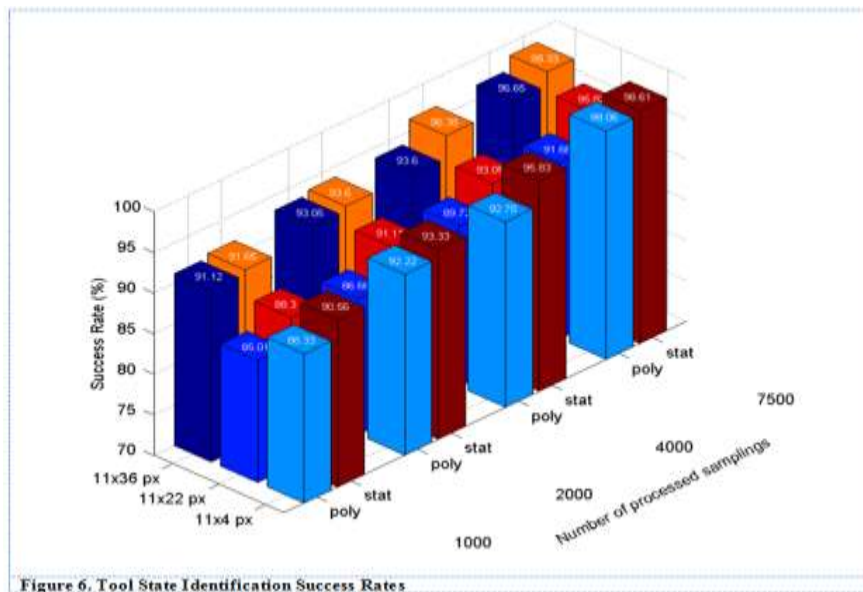


Figure 6. Tool State Identification Success Rates

The ability to be able to detect reliably when a tool bit has reached a the state of wear, where by the likelihood of predicting substandard work, expenditures of excess machine energy or the potential of catastrophic failure could thus lead itself to the production of a number of undesirable consequences. Environmental impacts that may be prevented by using this monitoring approach include parts rejection (waste), excess cutting friction (energy consumption, CO2 production, machine wear) and unplanned maintenance (loss of production time / output)

##### 4.2 Surface Roughness Assessment

In Tables 9 to 9, the R-values obtained from all the neural network configurations are reported. Each table reports results for one ROI. The best linear fitting in terms of R-value is reported in bold for each dataset, for the three ROIs respectively. The surface roughness assessment was carried out with R-values ranging from a minimum of 0.6367 to a maximum of 0.981. The average fitting R-value is 0.8793. This confirms that the features extracted with both methodologies are suitable for surface roughness assessment. Generally the statistical features lead to a better fitting, in fact the results show an average R-value equal to 0.9085 for statistical features against 0.8500 obtained using polynomial features.

The number of hidden layer nodes does not have a great impact on the results. The “low number” configurations (4-8 and 5-6) in fact, give better results than the “high number” configurations (4-16 and 5-18) with only a very small difference in R-value equal to 0.01. Best results are obtained extracting signals and features from the smallest ROI (11 x 4) showing an average fitting equal to 0.90. The fitting increases as the number of processed samplings increases. However, considering the 1000 samplings datasets, the surface roughness assessment can be carried out with R-values ranging from 0.6367 to 0.9448 (with an average R-value equal to 0.83). These results confirm the capability of the temperature to be a suitable quick indicator of the surface roughness. In Figures 7-9 the best fitting is reported for each ROI.

**Table 7.** 11x4 pixels ROI table of results

11x4 px			
1000 samplings			
Statistical Features		Polynomial Features	
Configuration	R	Configuration	R
4_8	<b>0.9227</b>	5_6	0.7214
4_16	0.9092	5_18	0.7413
2000 samplings			
Statistical Features		Polynomial Features	
Configuration	R	Configuration	R
4_8	0.9272	5_6	0.8864
4_16	<b>0.9716</b>	5_18	0.8488
4000 samplings			
Statistical Features		Polynomial Features	
Configuration	R	Configuration	R
4_8	0.8921	5_6	<b>0.9583</b>
4_16	0.9355	5_18	0.8502
7500 samplings			
Statistical Features		Polynomial Features	
Configuration	R	Configuration	R
4_8	<b>0.9811</b>	5_6	0.9445
4_16	0.9675	5_18	0.9803

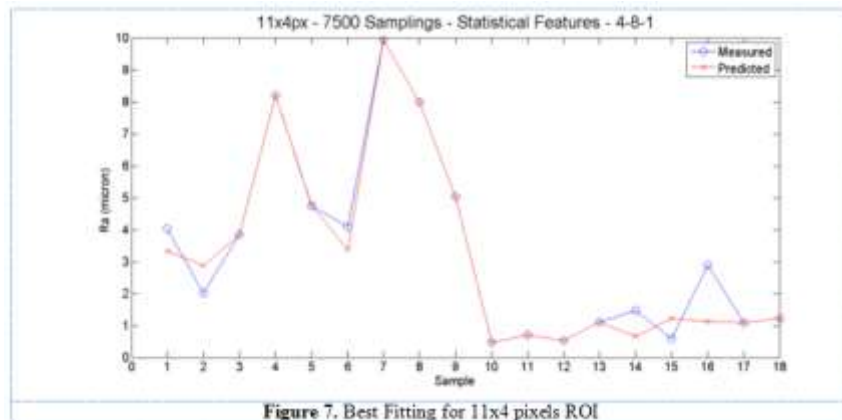


Figure 7. Best Fitting for 11x4 pixels ROI

**Table 8.** 11x22 pixels ROI table of results

11x22 px			
1000 samplings			
Statistical Features		Polynomial Features	
Configuration	R	Configuration	R
4_8	<b>0.8652</b>	5_6	0.7847
4_16	0.8259	5_18	0.6367
2000 samplings			
Statistical Features		Polynomial Features	
Configuration	R	Configuration	R
4_8	<b>0.8684</b>	5_6	0.811
4_16	0.8164	5_18	0.8666
4000 samplings			
Statistical Features		Polynomial Features	
Configuration	R	Configuration	R
4_8	<b>0.9363</b>	5_6	0.8275
4_16	0.9252	5_18	0.8289
7500 samplings			
Statistical Features		Polynomial Features	
Configuration	R	Configuration	R
4_8	<b>0.9097</b>	5_6	0.8647
4_16	0.9064	5_18	0.8463

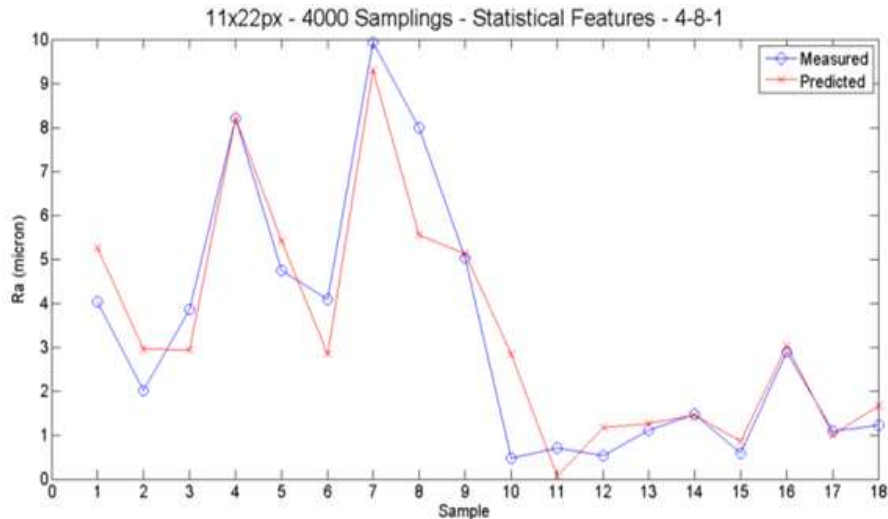


Figure 8. Best Fitting for 11x22 pixels ROI

Table 9. 11x36 pixels ROI table of results

11x36 px			
1000 samplings			
Statistical Features		Polynomial Features	
Configuration	R	Configuration	R
4_8	<b>0.9448</b>	5_6	0.8589
4_16	0.8808	5_18	0.8246
2000 samplings			
Statistical Features		Polynomial Features	
Configuration	R	Configuration	R
4_8	<b>0.9678</b>	5_6	0.9443
4_16	0.9134	5_18	0.9362
4000 samplings			
Statistical Features		Polynomial Features	
Configuration	R	Configuration	R
4_8	0.8458	5_6	0.8293
4_16	0.8431	5_18	<b>0.8903</b>
7500 samplings			
Statistical Features		Polynomial Features	
Configuration	R	Configuration	R
4_8	0.9128	5_6	0.8236
4_16	<b>0.9356</b>	5_18	0.8962

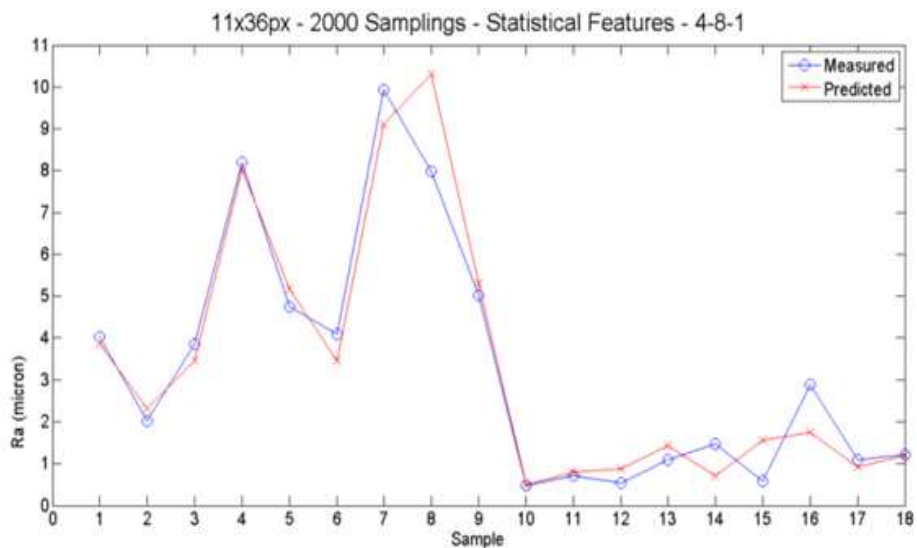


Figure 9. Best Fitting for 11x36 pixels ROI

The closeness of the relationship between temperature profile and the surface properties of the workpiece regardless of tool state provides potential opportunity to adjust the cutting parameters of the milling process in real time to maximise the rate of production (minimising energy) whilst ensuring desired surface finish is obtained (minimise reject and rework).

## V. CONCLUSIONS

Infrared monitoring of an aluminium milling process was performed to identify the tool wear state and to model the surface roughness. An experimental campaign of milling tests was carried out on an aluminium workpiece using a diverse range of cutting parameters. During machining, infrared temperature signals were acquired by using an infrared camera and surface roughness measurements were carried out after every cutting test on the milled surface. Signal processing procedures were implemented on infrared signals and two methodologies of signal features extraction were adopted, obtaining statistical features and polynomial coefficients features. An intelligent decision making support system was built for tool state identification through the implementation of Neural Networks Pattern Recognition. The results showed that both feature typologies are suitable for tool state identification with very high NN performance for decision making on cutting tool conditions during aluminium milling, but revealing a more reliable analysis from statistical features.

Moreover the Neural Network paradigm was applied to the signal features in order to assess the surface roughness and results showed that surface roughness assessment can be successfully carried out by monitoring temperature during milling. An efficient and effective monitoring system aimed at tool state identification and surface integrity requirements can improve environmental performances of machining operations by minimising the risk of dangerous faults which may damage the product. Also, avoiding additional operations due to non-acceptable tool conditions and surface finishing requirements helps in energy, time and resource saving. It is important to underline that prediction of tool wear and surface roughness plays a fundamental role in maintaining quality standards in machining processes while contributing to the reduction of environmental impact by optimising the utilisation of energy and resources. Future experimental research activities will involve similar methodology applied on different materials and machining processes to evaluate the applicability of the described technology and signal processing techniques for evaluating tool bit condition and production parameters in a range of manufacturing applications. Importantly, low cost IR sensors are required for sensing in the presence of cutting fluid in order to present an industry-ready monitoring technology.

## ACKNOWLEDGEMENTS

This research has been partially funded by the EPSRC Centre for Innovative Manufacturing in Industrial Sustainability (EP/I033351/1).

## REFERENCES

- [1]. M. F. Rajemi, P. T. Mativenga, and A. Aramcharoen, "Sustainable machining: Selection of optimum turning conditions based on minimum energy considerations," *J. Clean. Prod.*, vol. 18, no. 10–11, pp. 1059–1065, 2010.
- [2]. Y. Seow, S. Rahimifard, and E. Woolley, "Simulation of energy consumption in the manufacture of a product," *Int. J. Comput. Integr. Manuf.*, vol. 26, no. 7, pp. 663–680, 2013.
- [3]. Y. Luo, E. Woolley, S. Rahimifard, and A. Simeone, "Improving energy efficiency within manufacturing by recovering waste heat energy," *J. Therm. Eng.*, vol. 1, no. 5, p. 337, May 2015.
- [4]. D. Fratila, "Evaluation of near-dry machining effects on gear milling process efficiency," *J. Clean. Prod.*, vol. 17, no. 9, pp. 839–845, 2009.
- [5]. A. Devillez, F. Schneider, S. Dominiak, D. Dudzinski, and D. Larrouquere, "Cutting forces and wear in dry machining of Inconel 718 with coated carbide tools," *Wear*, vol. 262, no. 7–8, pp. 931–942, 2007.
- [6]. A. Rivero, L. N. López de Lacalle, and M. L. Penalva, "Tool wear detection in dry high-speed milling based upon the analysis of machine internal signals," *Mechatronics*, vol. 18, no. 10, pp. 627–633, 2008.
- [7]. R. Teti, K. Jemielniak, G. O'Donnell, and D. Dornfeld, "Advanced monitoring of machining operations," *CIRP Ann. - Manuf. Technol.*, vol. 59, no. 2, pp. 717–739, 2010.
- [8]. S. and S. R. S. Kalpakjian, *MANUFACTURING ENGINEERING* Illinois Institute of Technology. 2009.
- [9]. D. Kerr, J. Pengilley, and R. Garwood, "Assessment and visualisation of machine tool wear using computer vision," *Int. J. Adv. Manuf. Technol.*, vol. 28, no. 7–8, pp. 781–791, 2006.
- [10]. T. Segreto, A. Simeone, and R. Teti, "Sensor fusion for tool state classification in nickel superalloy high performance cutting," in *Procedia CIRP*, 2012, vol. 1, no. 1, pp. 593–598.
- [11]. F. Boud and N. N. Z. Gindy, "Application of multi-sensor signals for monitoring tool/workpiece

- condition in broaching,” *Int. J. Comput. Integr. Manuf.*, vol. 21, no. 6, pp. 715–729, 2008.
- [12]. M. A. Davies, T. Ueda, R. M’Saoubi, B. Mullany, and A. L. Cooke, “On The Measurement of Temperature in Material Removal Processes,” *CIRP Annals - Manufacturing Technology*, vol. 56, no. 2, pp. 581–604, 2007.
- [13]. H.-T. Young, “Cutting temperature responses to flank wear,” *Wear*, vol. 201, no. 1–2, pp. 117–120, 1996.
- [14]. T. Kitagawa, A. Kubo, and K. Maekawa, “Temperature and wear of cutting tools in high-speed machining of Incone1718 and Ti-6Al-6V-2Sn,” *Wear*, vol. 202, no. 2, pp. 142–148, 1997.
- [15]. F. Valiorgue, A. Brosse, J. Rech, H. Hamdi, J. M. Bergheau, F. Chinesta, Y. Chastel, and M. El Mansori, “Emissivity calibration for temperature measurement using infrared thermography in orthogonal cutting of 316L and 100Cr6 grinding,” in *International Conference on Advances in Materials and Processing Technologies (AMPT2010)*. AIP Conference Proceedings, 2011, vol. 1315, no. 1, pp. 1053–1058.
- [16]. G. Quintana, M. L. Garcia-Romeu, and J. Ciurana, “Surface roughness monitoring application based on artificial neural networks for ball-end milling operations,” *J. Intell. Manuf.*, vol. 22, no. 4, pp. 607–617, Oct. 2009.
- [17]. P. G. Benardos and G. C. Vosniakos, “Prediction of surface roughness in CNC face milling using neural networks and Taguchi’s design of experiments,” *Robot. Comput. Integr. Manuf.*, vol. 18, no. 5–6, pp. 343–354, 2002.
- [18]. M. Anuj Kumar Sehgal, “Optimized Prediction and Modeling Under End Milling Machining By ANOVA And Artificial Neural Network,” vol. Vol.2-Is, no. Vol.2-Issue 3 (March-2013), Apr. 2013.
- [19]. H. Oktem, T. Erzurumlu, and F. Erzincanli, “Prediction of minimum surface roughness in end milling mold parts using neural network and genetic algorithm,” *Materials & Design*, vol. 27, no. 9, pp. 735–744, 2006.
- [20]. U. Esme, A. Sagbas, and F. Kahraman, “Prediction of surface roughness in wire electrical discharge machining using design of experiments and neural networks,” *Iran. J. Sci. Technol. Trans. B, Eng.*, vol. 33, no. JUNE 2009, pp. 231–240, 2009.
- [21]. S. S. Lee and J. C. Chen, “On-line surface roughness recognition system using artificial neural networks system in turning operations,” *Int. J. Adv. Manuf. Technol.*, vol. 22, no. 7–8, pp. 498–509, Nov. 2003.
- [22]. Y.-H. Tsai, J. C. Chen, and S.-J. Lou, “An in-process surface recognition system based on neural networks in end milling cutting operations,” *Int. J. Mach. Tools Manuf.*, vol. 39, no. 4, pp. 583–605, Apr. 1999.
- [23]. K. A. Risbood, U. S. Dixit, and A. D. Sahasrabudhe, “Prediction of surface roughness and dimensional deviation by measuring cutting forces and vibrations in turning process,” *J. Mater. Process. Technol.*, vol. 132, no. 1–3, pp. 203–214, 2003.
- [24]. R. Azouzi and M. Guillot, “On-line prediction of surface finish and dimensional deviation in turning using neural network based sensor fusion,” *International Journal of Machine Tools and Manufacture*, vol. 37, no. 9, pp. 1201–1217, 1997.
- [25]. P. R. Aguiar, C. E. D. Cruz, W. C. F. Paula, and E. C. Bianchi, “Predicting surface roughness in grinding using neural networks,” *Adv. Robot. Autom. Control*, no. October, pp. 33–44, 2008.
- [26]. B. M. S. Lou, J. C. Chen, and C. M. Li, “Surface Roughness Prediction Technique For CNC End-Milling Surface Roughness Prediction Technique For CNC End-Milling,” *J. Ind. Technol.*, vol. 15, no. 1, pp. 1–6, 1999.
- [27]. C. H. Lauro, L. C. Brandão, and S. L. M. Ribeiro Filho, “Monitoring the temperature of the milling process using infrared camera,” *Sci. Res. Essays*, vol. 8, no. 23, pp. 1112–1120, 2013.
- [28]. J. Kodácsy and V. Molnár, “Investigation of cutting temperatures ’ relation to the tool wear,” *Ann. Fac. Eng. Hunedoara – Int. J. Eng.*, vol. IX, no. 2, pp. 169–172, 2011.
- [29]. A. I. Azmi, “Machinability study of fibre-reinforced polymer matrix composites.” *ResearchSpace@Auckland*, 2012.
- [30]. A. Simeone, E. B. Woolley, and S. Rahimifard, “Tool State Assessment for Reduction of Life Cycle Environmental Impacts of Aluminium Machining Processes via Infrared Temperature Monitoring,” *Procedia CIRP*, vol. 29, pp. 526–531, 2015.
- [31]. G. Wang, C. Liu, Y. Cui, and X. Feng, “Tool wear monitoring based on cointegration modelling of multisensory information,” *Int. J. Comput. Integr. Manuf.*, vol. 27, no. 5, pp. 479–487, 2014.
- [32]. A. Simeone, T. Segreto, and R. Teti, “Residual stress condition monitoring via sensor fusion in turning of Inconel 718,” in *Procedia CIRP*, 2013, vol. 12, pp. 67–72.
- [33]. T. Segreto, A. Simeone, and R. Teti, “Principal component analysis for feature extraction and NN pattern recognition in sensor monitoring of chip form during turning,” *CIRP J. Manuf. Sci. Technol.*,

vol. 7, no. 3, pp. 202–209, 2014.

- [34]. S. Haykin, “Neural Networks :,” Convergence, pp. 1–16, 1998.
- [35]. K. Levenberg, “A Method for the Solution of Certain Problems in Least Squares,” in *Quart. Appl. Math.*, 1944, vol. 2, pp. 164--168.
- [36]. D. W. Marquardt, “An Algorithm for Least Squares Estimation of Nonlinear Parameters,” *J. Soc. Ind. Appl. Math.*, vol. 11, no. 2, pp. 431–441, 1963.
- [37]. “<http://www.taylor-hobson.com/>,” 2015. .